On cascading failure models and robustness metrics in power networks

Nicolás Bordonaba Mateos

LUND UNIVERSITY

Department of Automatic Control

MSc Thesis
ISRN LUTFD2/TFRT--5997--SE
ISSN 0280-5316

Department of Automatic Control
Lund University
Box 118
SE-221 00 LUND
Sweden

Printed in Sweden by Tryckeriet i E-huset
Lund 2016

Abstract

Network research tries to give solutions within several areas, beginning from social interconnections, logistic problems, virus spreading, supply networks...etc. Some metrics have been developed in order to predict blackouts and improve power grid robustness. Metrics use part of the grid information seeking weakness without simulating the blackout process. On the other hand, simulation models unfold blackouts.

In this report, we study such metrics and models, seeking that model that could give us the most relevant information. The models studied in this report represent blackout as a branch breaking process, a singular line cut or a combination of line cuts might cause subsequent disconnections and unfold a blackout. The IEEE-14 and IEEE-96 RTS bus systems are used in order to simulate blackouts. Metrics suggestions are compared with the simulations in these grids in order to know which metric better captures the critical branches.

None of the studied metrics turns out to indicate always the worst blackout result as the first option. In addition, the results suggest that the effective resistance metric did not predict the critical transmission lines of the grid. Electrical betweenness and net-ability metrics obtain the critical transmission lines within their first suggestions. However, the results might be better if we also use other relevant information on the grid as the nominal power flow in each branch or the probability of having a line cut. Nevertheless, lines that carry a high amount of power flow are usually more protected and more difficult to being cut and develop a blackout. The probability of having a single line cut or a combination of line cuts will be useful in future assessments in order to seek not only the most critical branch cuts, but the most probable ones.

Acknowledgments

First of all I would like to express my gratitude towards those people that helped and supported me during this thesis. My greatest thanks go to my supervisor Giacomo and co-supervisor Carolina for supporting and advising me during this project every time I needed them. I would also like to thank my fellow students Demeter and Martino for great company and for helping me whenever I needed. Finally, my last gratitude goes to my family and Sarita that helped me from a distance in order to finish it abroad. Thank you everybody for every second you spent on me!

Nomenclature

Symbol	Description
$\mathscr{G}$	Undirected graph
n	Number of buses in graph $\mathscr{G}$
m	Number of branches in graph $\mathscr{G}$
$\mathscr{V}$	Set of nodes of $\mathscr{G}$
$\mathscr{E}$	Set of branches of $\mathscr{G}$
y_{ij}	Admittance of line $(i,j) \in \mathscr{E}$
r_{ij}	Resistance of line $(i,j) \in \mathscr{E}$
x_{ij}	Inductance of line $(i,j) \in \mathscr{E}$
b_{ij}	Susceptance of line $(i,j) \in \mathscr{E}$
g_{ij}	Conductance of line $(i,j) \in \mathscr{E}$
p_i	Active power in bus $i \in \mathscr{V}$
q_i	Reactive power in bus $i \in \mathscr{V}$
V_i	Voltage value in bus $i \in \mathscr{V}$
θ_i	Voltage phase in bus $i \in \mathscr{V}$
M	Incidence matrix
f	Power flow vector
p	Power injection vector
L	Set of load buses in $\mathscr{G}$
G	Set of generator buses in $\mathscr{G}$
X	Diagonal impedance matrix
θ	Phase angles vector
$c_{ij} = f_{ij}^{max}$	Capacity of line $(i,j) \in \mathscr{E}$
cf_P^i	Active power cost function of bus $i \in G$
cf_Q^i	Reactive power cost function of bus $i \in G$
V_i^{min}	Minimum voltage magnitude in bus $i \in \mathscr{V}$
V_i^{max}	Maximum voltage magnitude in bus $i \in \mathscr{V}$
θ_i^{min}	Minimum voltage phase in bus $i \in \mathscr{V}$
θ_i^{max}	Maximum voltage phase in bus $i \in \mathscr{V}$
p_i^{min}	Minimum active power in bus $i \in G$

p_i^{max}	Maximum active power in bus $i \in G$
q_i^{min}	Minimum reactive power in bus $i \in G$
q_i^{max}	Maximum reactive power in bus $i \in G$
B	Laplacian matrix
B^+	Inverse of the laplacian matrix using the Penrose pseudo-inverse operator
$R_{ij} = Z_j^i$	Effective resistance between node i and j
R_G	Effective graph resistance of $\mathscr{G}$ graph
μ_i	i^{th} eigenvalue of the B matrix
L_e	Electrical betweenness of line $e \in \mathscr{E}$
L_e^p	Positive electrical betweenness of line $e \in \mathscr{E}$
L_e^n	Negative electrical betweenness of line $e \in \mathscr{E}$
f_i^{gd}	Change of power flow in line i when injection on generator g and withdrawal at load d
C_g^d	Power transmission capacity
E	Efficiency
d_{ij}	Geodesic distance between buses i and j
N_G	Number of generators in $\mathscr{G}$ graph
N_L	Number of loads in $\mathscr{G}$ graph
A	Net-Ability metric
A_i	Net-Ability level when line i is cut
V_{A_i}	Vulnerability when line i is cut based on Net-Ability metric
$\mathscr{I}$	Island of $\mathscr{G}$ graph
p_{iDC}	Redispatched solution for flow conservation in power injection
p_{i0}	Initial power injection/withdrawal in node i before the blackout
h^0	Probability function in order to cut a transmission line that initiates the blackout in the OPA model
h^1	Probability function in order to cut a transmission line that is overloaded during the blackout in the OPA model
τ	Probability in order to cut a transmission line that initiates the blackout in the improved OPA model
ρ	Probability that OPA optimization take place in the improved OPA model
$\delta \left\lvert f_j/cj \right\rvert^u$	Probability function to cut a branch when is not overloaded in the improved OPA model
γ	Probability to cut a branch when is overloaded in the improved OPA model
β	Probability to cut a branch when is considered overloaded in the simplified improved OPA model
ξ	Probability to cut a branch when is overloaded in the simplified improved OPA model
D_L	Number of disconnected loads in a blackout
D_G	Number of disconnected generators in a blackout
$D_\mathscr{V}$	Number of disconnected buses in a blackout
$D_\mathscr{E}$	Number of disconnected branches in a blackout

LS	Load Shedding resulted from a blackout
p_i	Active power injection in generator bus i
p_{i0}	Nominal power injection in generator bus i in order to solve power flow problem
p_i^{final}	Final injection/withdrawal in bus i when a blackout occur
p_i^{max}	Maximum power injection in generator bus i
l_i	Initial demand in bus i
ϖ	Relation value between the nominal power injection in generation buses and their maximum power allowed to inject
f_0	Nominal power flow array
υ	Relation value between the nominal power flow in each branch and their maximum power flow allowed

Contents

1

Introduction

Electric power systems are important critical infrastructures that support our economy and social structure [16]. A power disconnection in a grid could affect urban transportation systems, heating and cooling systems, computer systems, factories, communication systems, hospitals, and a huge part of the economic activity. In our common life we use electricity daily and the real cost of large blackouts is impossible to measure.

High-voltage transmission systems are designed as a grid with multiple paths between loads and generators. New renewable energies and increased demand are stressing these grids, adding more volatility to the power grids' behavior. A blackout can be described as a branch breaking process. The causes that initiate this process are not complex, but huge in quantity. They can be described as natural and human disturbances as in [17]:

Natural disturbances: e.g, Ice storms, hurricanes, tornadoes, earthquakes.

Human disturbances: e.g, Human accidents, equipment failures, cyber attacks.

In 2003, a major blackout occurred in Southern Sweden and Eastern Denmark. The coincidence of several faults lead to an excess in the system far above the contingencies and security standards [18]. On the other hand, another example, caused by a combination of natural and human disturbances occurred in North America in 2003 when high-current arcs where generated between some transmission lines and nearby trees [17]. The inadequate vegetation management and the growth of trees generated this blackout. The number of possible causes increases with the power grid complexity.

Blackout usually occur as the outcome of a series of failures in the power network. Understanding and controlling these cascading mechanisms has became a

central research problem [22]. In this report blackout in the power network is described as a branch breaking process, whereby, branches could became inactive and unfold other line cuts. Hence, due to some of the above disturbances a branch might be cut and initiate a power flow redistribution through the network that could affect other transmission lines. Subsequently, some lines could be overloaded and cut. Some examples of blackout models as a branch breaking processes are [8], [9], [10], [11], [12] and [13]. In conclusion, it is important to try to prevent blackouts by studying the behavior of these complex phenomena.

1.1 Purpose

The aim of this Thesis is to explain some basic concepts of the blackout and to compare different metrics that try to predict critical blackout results. Using blackout models we can simulate the behavior of this process, therefore, we compare different models that represent blackouts as branch breaking processes. Metrics try to simplify the complexity of grids based on their measured parameters and to obtain some relevant information. In this report the results of the simulations are compared with the metric suggestions seeking for the most critical transmission lines in the system.

1.2 Goals

Study metrics that try to capture important characteristics of the network in order to predict blackouts

Study models of a branch breaking process that try to simulate the nature of the blackout and decide on one of them to compare metrics and simulation results

Analyze which metric has better results compared with the simulations

1.3 Disposition

First of all, in Chapter 2 we explain the Direct Current(DC) power flow simplification of a power grid. We also describe metrics that use measured parameters of the grid in order to capture the critical transmission lines. Furthermore, some blackout models will be presented and compared. One of these models that represents blackouts as a branch breaking process will be used in all the following simulations.

Moreover, in Chapter 3 different simulations will be done using IEEE-14 and IEEE-96 RTS bus systems. The blackout results from cutting a singular branch

is compared with the metrics suggestions. Therefore, the critical branches, those which unfold the severe blackouts, should be captured by the studied metrics.

2

Background

In this chapter the DC power flow model is introduced as an approximation of the AC power flow model. This model simplifies power grid equations, therefore, it will be easier to simulate blackouts. Furthermore, the transmission line capacities and the Optimal Power Flow(OPF) are slightly explained. Moreover, three metrics that seek the critical transmission lines in a power grid are described. Finally, some blackout models based on branch breaking process are explained in order to seek one of them and use it in the following simulations.

2.1 DC power flow model

Let $\mathscr{G} = (\mathscr{V}, \mathscr{E})$ be an undirected graph. $\mathscr{V} := \{1, 2, ..., n\}$ will be the set of nodes that represent buses and $\mathscr{E} := \{1, 2, ..., m\}$ will be the set of edges that represent transmission lines or branches in a power grid. Each edge $e \in \mathscr{E}$ can be given an arbitrary orientation as $(i, j) \in \mathscr{E}$ which is directed from i to j and $i, j \in \mathscr{V}$.

For each transmission line $e = (i, j) \in \mathscr{E}$ we have a resistance r_{ij} and an inductance x_{ij}, therefore the admittance, the susceptance and the conductance of branch e as y_{ij}, b_{ij} and g_{ij} respectively are termed below:

$$y_{ij} = \frac{1}{r_{ij} + x_{ij}\mathrm{j}}; \quad b_{ij} = \left|y_{ij}\right| \sin\left(\arg\left(y_{ij}\right)\right); \quad g_{ij} = \left|y_{ij}\right| \cos\left(\arg\left(y_{ij}\right)\right)$$

$$y_{ij} = g_{ij} + b_{ij}\mathrm{j}$$

Each bus $i \in \mathscr{V}$ has an active power value p_i, a reactive power value q_i a voltage magnitude V_i and a voltage phase θ_i. The AC power flow model represents the power grid behavior as is described in [1] and [2]:

$$p_i = \sum_{j=1}^{n} \sum_{j \neq i} |V_i|^2 g_{ij} - |V_i| |V_j| \{ \ g_{ij} \cos(\theta_i - \theta_j) + b_{ij} \sin(\theta_i - \theta_j) \ \} \quad (2.1)$$

$$q_i = \sum_{j=1}^{n} \sum_{j \neq i} - |V_i|^2 b_{ij} - |V_i| |V_j| \{ \ -b_{ij} \cos(\theta_i - \theta_j) + g_{ij} \sin(\theta_i - \theta_j) \ \} \quad (2.2)$$

At this point some assumptions are needed in order to develop the DC model:

1. The resistance of transmission circuits is significantly less than the impedance. As a result the admittance is computed using only the impedance and the conductance is 0.

$$r_{ij} \ll x_{ij} \rightarrow \quad b_{ij} \approx -\tfrac{1}{x_{ij}} \quad g_{ij} \approx 0$$

$$p_i \approx \textstyle\sum_{j=1 \ j \neq i}^{n} - |V_i| |V_j| \{ \ +b_{ij} \sin(\theta_i - \theta_j) \ \}$$

$$q_i \approx \textstyle\sum_{j=1 \ j \neq i}^{n} - |V_i|^2 b_{ij} - |V_i| |V_j| \{ \ -b_{ij} \cos(\theta_i - \theta_j) \ \}$$

2. The difference between phase angles of connected buses is sufficiently small. Then, the cosine of the difference is close to one and the sine of the difference is approximated to the difference value:

$$\theta_i \approx \theta_j \rightarrow \quad \cos(\theta_i - \theta_j) \approx 1 \quad \sin(\theta_i - \theta_j) \approx (\theta_i - \theta_j)$$

$$p_i \approx \textstyle\sum_{j=1 \ j \neq i}^{n} - |V_i| |V_j| \{ \ +b_{ij} (\theta_i - \theta_j) \ \}$$

$$q_i \approx \textstyle\sum_{j=1 \ j \neq i}^{n} - |V_i|^2 b_{ij} - |V_i| |V_j| \{ \ -b_{ij} \ \}$$

3. The numerical values of voltage magnitudes in every bus are unity:

$$|V_i| = 1 \quad \forall i \in \mathscr{E}$$

$$p_i \approx \textstyle\sum_{j=1 \ j \neq i}^{n} -b_{ij} (\theta_i - \theta_j)$$

$$q_i \approx 0$$

As a consequence of applying the assumptions of fast decoupled and DC power flow, the active power is bigger than the reactive power in each bus: $P_i \gg Q_i$. Hence a two non-linear functions problem is solved as a one linear function problem. The active power is calculated as below:

$$p_i \approx \sum_{j=1 \; j \neq i}^{n} + \frac{1}{x_{ij}} (\theta_i - \theta_j)$$

In order to rewrite the DC power flow model in a more compact way we introduce all the necessary vectors and matrices below as in [20]:

Incidence matrix $M : n\text{x}m$.
For each branch $e = (i, j)$, where $i, j \in \mathscr{V}$, $M_{ie} = +1$ and $M_{je} = -1$.

$$M_{ie} = \left\{ \begin{array}{cc} +1 & e = (i, j) \\ -1 & e = (j, i) \\ 0 & otherwise \end{array} \right\}$$

Power flow vector $f : m\text{x}1 = (f_e : e \in \mathscr{E})$.
f_e represents the power flow of transmission line e.

Power injection vector $p : n\text{x}1 = (p_i : i \in \mathscr{V})$.
p_i represents the injection or withdrawal of bus i. Because of the flow conservation the sum of all the entries is zero $\sum_{i=1}^{n} p_i = 0$. Below load and generator buses are described:

$$L(p) := \{i \in \mathscr{V} : p_i < 0\} \quad G(p) := \{i \in \mathscr{V} : p_i > 0\}$$

Diagonal impedance matrix $X : m\text{x}m$.
Each entry $X_{ee} = x_{ij}$. Where x_{ij} is the impedance between bus i and bus j and $e = (i, j) \in \mathscr{E}$ is the transmission line that connect that nodes.

Phase angles vector $\theta : n\text{x}1 = (\theta_i : i \in \mathscr{V})$.
θ_i represents the voltage phase of node i.

Finally the DC model is computed assuming a fixed p and θ (reference bus) $= 0$ using flow conservation:

$$Mf = p \tag{2.3}$$
$$Xf = M'\theta \tag{2.4}$$

The resulting f and θ vectors are the power flow solution. As relevant detail of this model is the similitude between the equations below:

$$f_{ij} = \frac{\theta_i - \theta_j}{x_{ij}} \quad \rightarrow \quad I = \frac{\Delta U}{R}$$

This is why this approximation to the AC model is called DC model.

2.2 Transmission lines capacities

A blackout can be described as a breaking branches process. Hence it is necessary to declare transmission line capacities. These boundaries represent the maximum permitted power flow that each transmission line can carry symmetrically in negative or positive value:

$$c_{ij} = c_e = f_{ij}^{max} = f_e^{max} \geq \left| f_{ij} \right| \quad \forall e = (i,j) \in \mathscr{E}$$

Thereby, the blackout phenomena are developed due to the existence of these capacities. If any branch exceeds its own c_{ij} value, it will be overloaded and cut. The blackout models described later in this report are based on the existence of these limits: [8], [9], [10], [11], [12] and [13].

2.3 Optimal Power Flow (OPF)

In normal operation state the power flow problem is solved based on economic and security factors as described in [2], [21] and [23]. Hence, the power generated is measured in economic terms and by paying attention to the system boundaries. Therefore, the objective function is a summation of individual polynomial cost functions cf_P^i and cf_Q^i of real and reactive power injections for each generator respectively. This is the OPF problem for the AC power flow model where f_{ij} is composed by active and reactive power flow:

$$\begin{array}{lcc}
\text{minimize} & \sum_{i \in G} cf_P^i(p_i) + cf_Q^i(q_i) & \forall i \in G \\
\text{subject to:} & \left| f_{ij} \right| \leq f_{ij}^{max} & \forall (i,j) \in \mathscr{E} \\
& V_i^{min} \leq |V_i| \leq V_i^{max} & \forall i \in \mathscr{V} \\
& \theta_i^{min} \leq \theta_i \leq \theta_i^{max} & \forall i \in \mathscr{V} \\
& p_i^{min} \leq p_i \leq p_i^{max} & \forall i \in G \\
& q_i^{min} \leq q_i \leq q_i^{max} & \forall i \in G \\
& \text{Equation (2.1)} & \forall i \in \mathscr{V} \\
& \text{Equation (2.2)} & \forall i \in \mathscr{V} \\
& \theta\,(\text{reference bus}) = 0 &
\end{array}$$

Here $|V_i|$ and q_i is the voltage magnitude and reactive power of bus i. While, the reference bus is the only node where the voltage phase is known and referring to these value we can get the remaining values. This optimization is subject to the AC power flow model. When we work with the DC power flow model the OPF is simplified too. It will not depend on voltage magnitude and reactive power:

$$\begin{array}{lcc} \text{minimize} & \sum_{i \in G} c f_P^i(p_i) & \forall i \in G \\ \text{subject to:} & |f_{ij}| \leq f_{ij}^{max} & \forall (i,j) \in \mathscr{E} \\ & \theta_i^{min} \leq \theta_i \leq \theta_i^{max} & \forall i \in \mathscr{V} \\ & p_i^{min} \leq p_i \leq p_i^{max} & \forall i \in G \\ & Mf = p & \\ & Xf = M'\theta & \\ & \theta\,(\text{reference bus}) = 0 & \end{array}$$

In this case, the optimization is also subject to the DC power flow model, given by equations (2.3) and (2.4). In the OPF model the active power in generation buses is treated as variables and in load buses as constants. Therefore, the minimization function aim is to allow a proper power injection in generation with assuming a fixed demand in all load buses.

If this model is used assuming an initial line cut, the result of the optimization might be infeasible. This is due to that one or more capacities will be meet. In this case, any information about the following cut lines can not be retrieved. While if no blackout is unfolded the result is feasible. Consequently, this model is satisfactory for normal operational problems, despite not being able to represent the blackout activity correctly.

2.4 Network metrics

The topological complex network based metrics fall short in order to predict power grid robustness against blackouts as declared in [3], [4] and [5]. "Net-ability" and "electrical betweenness" are some extended topological metrics. The aim of these contributions is that the pure topological metrics ignore the electrical properties and the working boundaries of networks. In addition, the topological metric "effective resistance" uses the electrical relation between buses to describe the vulnerability of a grid. Hence, all these metrics are based on electrical factors in order to measure power grid robustness.

Effective resistance

The effective resistance measures the differential potential between two nodes when a unit of current goes from one bus to the other [6, 7]. In order to get this value

we could use the Laplacian matrix. This matrix is constructed by the impedances of the transmission lines as follows:

Laplacian matrix $B : nxn$.

$$B_{ij} = \left\{ \begin{array}{ll} \frac{-1}{x_{ij}} & i \neq j \\ \sum_{k \neq i} \frac{+1}{x_{ik}} & i = j \end{array} \right\}$$

The effective resistance between two nodes could be computed as described in [6,7]:

$$R_{ij} = B^{+}_{ii} + B^{+}_{jj} - 2B^{+}_{ij}$$

The B^{+} is the inverse matrix of B using the Penrose pseudo-inverse operator. It is also possible to calculate the effective resistance between node i and j using the differential potential between two nodes. In Figure 2.1 is shown an example in order to calculate the effective resistance between two buses:

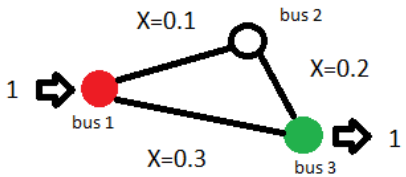

$$p = \begin{pmatrix} +1 \\ 0 \\ -1 \end{pmatrix} \quad M = \begin{pmatrix} 1 & 1 & 0 \\ -1 & 0 & 1 \\ 0 & -1 & -1 \end{pmatrix} \quad X = \begin{pmatrix} 0.1 & 0 & 0 \\ 0 & 0.3 & 0 \\ 0 & 0 & 0.2 \end{pmatrix}$$

Figure 2.1 Example with a triangular bus system used to show how to calculate the effective resistance between two buses. The red bus is injects a unity of injection and the green bus demand a unity of withdrawal. It is also show the p array and the M and X matrix.

A fixed p vector with 0 in all its entries except for the i^{th} and the j^{th} entries (in this case the red and green buses), with 1 and -1 as values respectively. Then, with this fixed p and $\theta\,(\text{bus } 1) = 0$, θ and f arrays are calculated using the DC power flow model (Equations (2.3) and (2.4)):

$$f = \begin{pmatrix} 0.5 \\ 0.5 \\ 0.5 \end{pmatrix} \quad \theta = \begin{pmatrix} 0 \\ -0.05 \\ -0.15 \end{pmatrix}$$

Finally, the effective resistance between the red and the green bus in Figure 2.1 will be computed as the difference between voltage phases of these two buses. Therefore, the effective resistance between them is equal to 0.15.

The effective graph resistance is defined as the sum of all the effective resistances [6,7]:

$$R_G = \sum_{i=1}^{n} \sum_{j=i+1}^{n} R_{ij}$$

In the network of Figure 2.1 it is necessary to calculate R_{12} and R_{23}. In this case $R_{12} = 0.083$ and $R_{23} = 0.133$, therefore the effective graph resistance will be $R_G = 0.366$. This can also be calculated using the eigenvalues [6,7] of the Laplacian matrix B, where μ is a non zero eigenvalue of B:

$$R_G = n \sum_{i=1}^{n-1} \frac{1}{\mu_i}$$

The electrical topology of a power grid has a major importance in the network dynamics rather than the physical topology. Therefore, the effective resistance between two buses represents the equivalent impedance between them. A higher number of possible paths between two nodes will represent robustness, because in case of a link failure, power flow will be easily redispatched into other paths. A consistent distribution of the impedance values will also result in a more robust grid. In these cases where the number of paths between nodes is higher and the impedances are similarly organized the computed value of the effective graph resistance is smaller.

Electrical betweenness

This metric is the sum of branches' sensitivity to the change of power injection/withdrawal, weighted by the capacity of relevant transmission lines. Each branch will be represented by a single electrical betweenness value, the higher it is the more critical the branch is. As is described in [3] the electrical betweenness of each line is defined as follows:

$$L_i = \max \left[\left| L_i^p \right|, \left| L_i^n \right| \right] \quad \forall i \in \mathscr{E}$$

Here L_i^p and L_i^n represent the positive and negative electrical betweenness respectively, depending on the sign of the resulting f_i^{gd}:

$$\begin{array}{ll} L_i^p = \sum_{g\in G}\sum_{d\in L} C_g^d f_i^{gd} & \text{where the sum is taken over terms when } f_i^{gd} > 0 \\ L_i^n = \sum_{g\in G}\sum_{d\in L} C_g^d f_i^{gd} & \text{where the sum is taken over terms when } f_i^{gd} < 0 \end{array}$$

Considering g as an injection bus generator and d as a withdrawal bus load the power transmission capacity C_g^d is the power injected by g when the first line reaches its limit. f_i^{gd} is the change of power flow in line i when injection is on generator g and withdrawal at load d. In order to calculate these values it is necessary to solve the power flow problem, where $p_g = 1$, $p_d = -1$ and for all the remaining entries $p_i = 0$:

$$\begin{gathered} Mf^{gd} = p \\ Xf^{gd} = M'\theta^{gd} \\ \theta(\text{reference bus}) = 0 \end{gathered}$$

Thereby, C_g^d is calculated as follow:

$$C_g^d = \min\left\{\frac{f_1^{max}}{\left|f_1^{gd}\right|}, \ldots, \frac{f_m^{max}}{\left|f_m^{gd}\right|}\right\}$$

Here f_e^{max} is the capacity of line e. Hence, it is necessary to calculate branch power flows for each combination of generators and loads, capture the most stressed transmission line and weight each line power flows with the transmission capacityC_g^d. Figure 2.2 unfolds an example of this calculation:

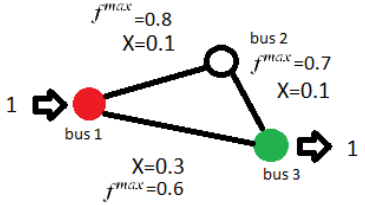

$$f = \begin{pmatrix} f_{1,2} = 0.6 \\ f_{1,3} = 0.4 \\ f_{2,3} = 0.6 \end{pmatrix} \quad C_1^3 = \min\left\{\frac{0.8}{0.6}, \frac{0.6}{0.4}, \frac{0.7}{0.6}\right\} = \frac{0.7}{0.6} \quad L^p = \begin{pmatrix} 0.7 \\ 0.466 \\ 0.7 \end{pmatrix} \quad L^n = \begin{pmatrix} 0 \\ 0 \\ 0 \end{pmatrix}$$

Figure 2.2 Example with a triangle bus system used to show how to calculate the electrical betweenness. The red and the green buses are the only generator and load respectively. For each branch there is a capacity and an impedance value. Here f is the power flow array from the DC model solution, while C_1^3, L^p and L^n are the transmission capacity of generator bus 1 and load bus 3 and, the negative and positive electrical betweenness respectively. The more critical branches are (1,2) and (2,3).

Electrical betweenness metric L_i indicates the criticality of branch i. Hence, a transmission line will be more critical as this metric is higher. Therefore, in this example the most critical branches are transmission lines (1,2) and (2,3).

Net-ability

The net-ability metric described in [4] is extended from efficiency considering electric distance and line flow limits. The efficiency E quantifies the overall performance of a network as the mean geodesic distance over all pairs of buses in the network:

$$E = \frac{1}{N_G N_L} \sum_{i \neq j \in \mathcal{V}} \frac{1}{d_{ij}}$$

Here d_{ij} is the geodesic distance defined as the number of branches in the shortest path between i and j buses, while N_G and N_L are the total number of generator and load buses respectively. As is described above, the net-ability metric is calculated considering electrical distance Z_g^d and line flow limits C_g^d:

$$A = \frac{1}{N_G N_L} \sum_{g \in G} \sum_{d \in L} \frac{C_g^d}{Z_g^d}$$

Here C_g^d is the power transmission capacity defined in the electrical betweenness point and Z_g^d is the effective resistance between nodes g and d already described:

$$Z_g^d = R_{gd}$$

In addition, the vulnerability of line i is defined as the net-ability decrease caused by a cut in line i:

$$V_{Ai} = \frac{A - A_i}{A}$$

Here A_i is the net-ability level when line i is cut. Hence the most critical edge has the highest value of V_{Ai} and the lowest value of A_i.

Remark

It is necessary to emphasize that, with the metrics described, there are two ways to measure robustness:

1. The vulnerability of a grid in its normal working state when an individual transmission line is cut.

2. The robustness of a grid against blackout attacks when an individual branch is added to the structure.

In one case the robustness is seen as an attack to a static grid and on the other hand the second point adds the idea of improvement from the initial state. The electrical betweenness is not able to measure this second kind of robustness because it has focused on the branch significances on the grid. However, the other two metrics (effective resistance and net-ability) can be used in both cases as they try to measure the structural robustness when some alteration takes place in the grid. In this report, we will focus on the first point. Moreover, a simple example is shown in order to see how each metric could have different results:

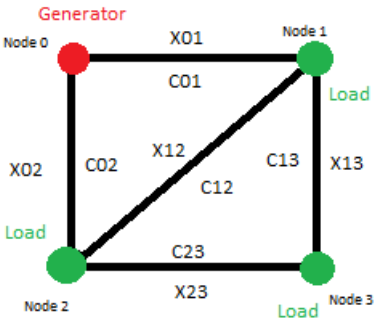

Figure 2.3 Example with a square bus system used to show the differences between metrics

$$X_{01} = 0.4 \quad X_{02} = 0.3 \quad X_{12} = 0.04 \quad X_{23} = 0.4 \quad X_{13} = 0.1$$
$$C_{01} = 3 \quad C_{02} = 0.4 \quad C_{12} = 1 \quad C_{23} = 1 \quad C_{13} = 2$$

The metrics described in this point are applied using the power grid in Figure 2.3 with the transmission line data above. Furthermore, the results are different for each metric, showing that they could obtain distinct transmission lines in looking for the critical branches:

Metric	Electrical Betweenness	Effective resistance	Net-ability
Critical branch	0-2	1-3	0-1

Table 2.1 Figure 2.3 critical branch suggestions using different metrics

2.5 Blackout models

Blackouts can occur from many causes. Nodes in models represent generators and loads that can fail and develop a blackout. However, in this report, we will study the blackouts as a breaking branch process. In the models explained below the blackout starts with a branch cut that develops other transmission line cuts and the subsequent blackout. In a real power grid at least a N-1 level of security is used. This means that it is impossible for a blackout to occur with a single branch cut as is explained in [14].

In this section a blackout characterization and some blackout models based on a branch breaking process are described. First of all, we describe the blackout characterization. Secondly, we introduce the Static model that is the most simple example

of a blackout model that we could develop. Furthermore, two more blackout models are taken into consideration in this assessment. Finally, we will decide to use one of these models in the following simulations.

Blackout characterization

In order to classify and delimit the criticality between different blackouts it is necessary to enumerate the distinct blackout levels. Furthermore, we define the following terms:

number of disconnected loads	D_L
number of disconnected generators	D_G
number of disconnected buses	$D_{\mathscr{V}} = D_G + D_L$
number of disconnected lines	$D_{\mathscr{E}}$

$$\text{load shedding} \quad LS = \frac{\Sigma_{i \in L}\left(p_i^{final} - p_{i0}\right)}{\Sigma_{i \in L}(-p_{i0})} \tag{2.5}$$

Here p_{i0} and p_i^{final} are the initial and the final withdrawal in the load bus i during the blackout. Therefore, the LS result will be the proportion of demand in loads that can not be supported by generators when the blackout has occurred. In order for the importance on demand on loads to prevail over the rest, the classification is simplified using these two terms: D_L and LS. This characterization is enumerated from the less important to the more significant blackout:

No blackout $LS = 0$, $D_L = 0$, $D_{\mathscr{E}} \geq 0$, and $D_G \geq 0$
When some lines and generators could be disconnected but no load is disjointed from the network and no load shedding exists.

Small blackout $LS > 0$, $D_L = 0$, $D_{\mathscr{E}} \geq 0$, and $D_G \geq 0$
When some load shedding happens without any load disconnection.

Intermediate blackout $LS > 0$, $D_L > 0$, $D_{\mathscr{E}} \geq 0$, and $D_G \geq 0$
Some load shedding and load bus disconnection take place in a blackout.

Total blackout $LS = 1$
No load bus is connected to any generator. The blackout is complete.

In summary, given the Load Shedding value LS the impact of the blackout can be correctly characterized. Blackouts will be categorized as more critical when LS is higher.

Static model

In the Static model the power flows are calculated directly using the DC power flow equations and if any flow exceeds the capacity of its branch, this transmission line is cut. There is no upper bound on the amount of energy that generators can supply and loads have their initial values if they are still connected to the grid, and zero if they are disconnected. If a load is still connected to a generator it is still joined to the grid. Capacities are sufficient in order to maintain a normal operation mode. Therefore, it is necessary to cut an initial transmission line for a blackout to occur. First, we will describe the static model procedure using an example and then the algorithm will be detailed.

Figure 2.4 will be used in order to explain the Static model. As seen in (a) there are four buses, one generator with +1 as injection and one load with -1 as withdrawal. There are also five branches with different capacity values (C01, C02, C12, C13 and C23) and three possible conductivity values (A, B and 1). The conductivity value is the inverse of the impedance in lines, therefore, a higher conductivity will represent a relative increase of power flow in that branch. In this example A and B are considered higher than 1. As said above, all branches have sufficient capacity to work correctly in normal grid operation. The power flow within all the branches of Figure 2.4 (a) are below:

$$f_{01} = \frac{B+A}{AB+B+2A} \quad f_{02} = \frac{AB+A}{AB+B+2A} \quad f_{12} = \frac{-AB+B}{AB+B+2A}$$

$$f_{23} = \frac{A+B}{AB+B+2A} \quad f_{13} = \frac{A+AB}{AB+B+2A}$$

In this model if any branch has exceeded its capacity $c_{ij} < f_{ij}$ it will be cut. As written above the capacities are enough to support normal operation values, therefore, it is necessary to cut a line in order to unfold a blackout. Furthermore, as seen in Figure 2.4(b) the 1-3 branch is triggered and the power flow has a new solution:

$$f_{01} = \frac{B}{AB+B+2A} \quad f_{02} = \frac{AB+A}{AB+B+2A} \quad f_{12} = \frac{B}{AB+B+2A} \quad f_{23} = 1$$

Here the 2-3 branch has increased its power flow and also 1-2 line could have increased its flow (depending on A and B values). Therefore, the case where $|f_{23}| > C23$ & $|f_{12}| < C12$ is shown in (c) and the disconnection between generator and load is complete. However, there is also the possibility that $|f_{23}| < C23$ & $|f_{12}| > C12$ and it will result in Figure 2.4(d):

$$f_{01} = 0 \quad f_{02} = 1 \quad f_{23} = 1$$

At this point in Figure 2.4(d) it is assumed that $1 < C23$. Therefore, the only possible transmission line that could be cut is the 0-2 branch which is the only line that has increased its flow. In this case the disconnected graph is shown in Figure 2.4(e).

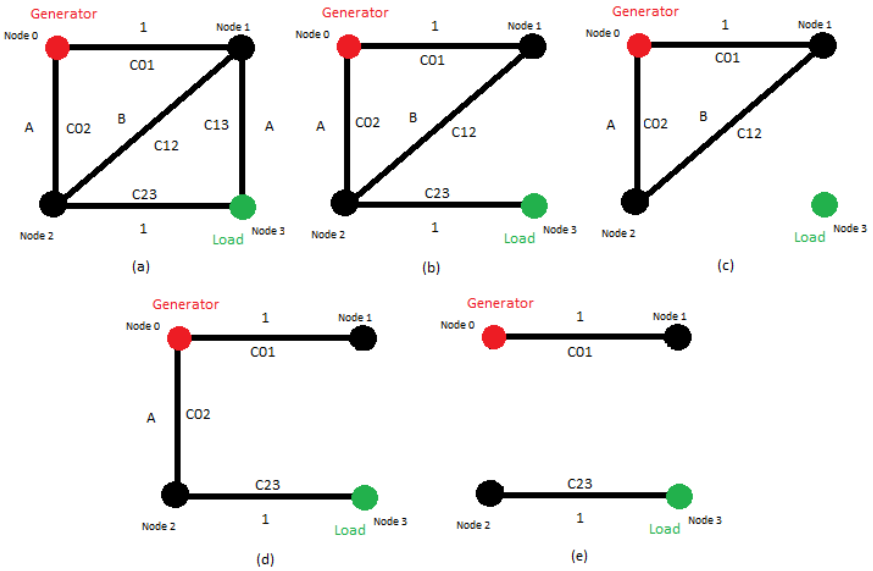

Figure 2.4 Static model example when 1-3 branch is cut

In this example, there is only one generator and load, thereby when they are disconnected power injection and withdrawal will be 0 respectively. However, it is necessary to recalculate the power injections if there are more loads and generators with an initial power injection/withdrawal and some of these loads or generators were disconnected. The load withdrawals never change their values if they are still connected to some generators and there is no limit in power generator injections. Furthermore, the injection increase or decrease is assumed to be shared homogeneously between all generators, in order to get the most probable option. It could be possible to generate islands with generators and loads disconnected between them, thus, the power injection is calculated with the buses of each island. In conclusion, it can be stated that the Static model uses the DC power flow problem without any boundaries, maintaining the initial demand in loads and redistributing proportionally the power injected by the generators.

In addition, Figure 2.5 represents an initial square grid in Figure 2.5(a) and the same grid with an additional grid between nodes 1 and 2 in Figure 2.5(b). As in the example below the power injection in node 0 is +1 and the withdrawal in node 3 is -1. Although in this example $A < 1$ and $B > 1$. Moreover, the power flow results in Figure 2.5(a) is below:

$$f_{01} = \frac{1}{2} \quad f_{02} = \frac{1}{2} \quad f_{23} = \frac{1}{2} \quad f_{13} = \frac{1}{2}$$

Consequently, the A value does not change the power flow in Figure 2.5(a). After adding the 1-2 branch the power flow will be:

$$f_{01} = \frac{B+A}{AB+B+2A} \quad f_{02} = \frac{AB+A}{AB+B+2A} \quad f_{12} = \frac{-AB+B}{AB+B+2A}$$

$$f_{23} = \frac{A+B}{AB+B+2A} \quad f_{13} = \frac{A+AB}{AB+B+2A}$$

Here $f_{01} = f_{23} > f_{02} = f_{13}$ and $f_{01} = f_{23} > \frac{1}{2}$. Thereby, in this example it is shown that by adding a new line it is possible to increase power flow on other lines. These lines can be more stressed, thus, adding one line in order to improve robustness could be damaging as a blackout unfolds. In summary, power grids behavior is complex and very difficult to predict when complexity increases.

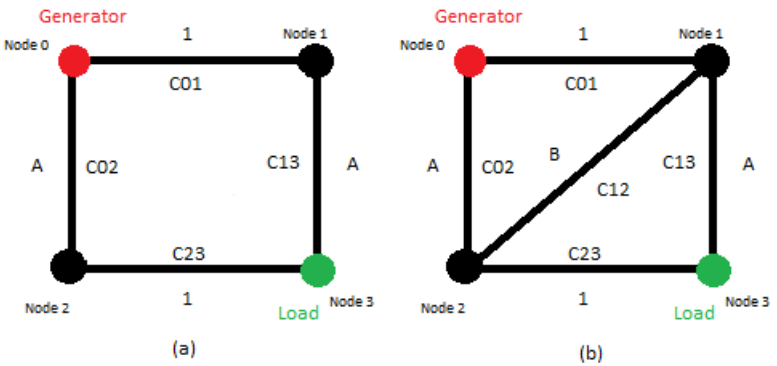

Figure 2.5 Static model example when 1-2 branch is added. It illustrates that adding a line can increase power flow on other lines, and initiate a power collapse.

Therefore, as described above the algorithm of this model works as follows:

1. It is decided to cut one line.

2. In this point some loads, generators or a set of both could be disconnected from the network. In other words, if some loads are not connected to any generator and/or some generators are not linked with any load bus then these nodes are disconnected from the entire network. It is understood that the grid could evolve into different sets of networks with generators and loads. Let $\mathscr{I}$ be an island of graph $\mathscr{G}$. Hence, in each island the power generation is calculated as below:

$$\forall \mathscr{I} \in \mathscr{G}$$

$$p_{iDC} = p_{i0} - \frac{-\sum_{j \in L \cap \mathscr{I}} p_{j0} - \sum_{j \in G \cap \mathscr{I}} p_{j0}}{\text{number of buses in } G \cap \mathscr{I}} \quad \forall i \in G \cap \mathscr{I}$$

$$p_{iDC} = p_{i0} \quad \forall i \in L \cap \mathscr{I}$$

This is the most simplest algorithm in order to recalculate power injection, it is proportional to the initial power injection. Here p_{i0} is the initial power injection/withdrawal in node i before any line is cut. While p_{iDC} is the re-dispatched power injection in bus i in order to achieve flow conservation. With p_{DC} values the DC power flow solution is reachable. If some buses are disconnected due to the blackout this formula allows the power injection in generators to be redistributed with the same cost.

3. The DC power flow is calculated:

$$\begin{gathered} Mf = p_{iDC} \\ Xf = M'\theta \\ \theta(\text{refbus}) = 0 \end{gathered}$$

4. If in some line the power flow exceeds its capacity $f_{ij} > c_{ij}$ this line will be cut and step 2 will be repeated. If no line is overloaded the blackout is finished.

OPA model

The ORNL-PSerc-Alaska (OPA) model is developed in [8], [9], [10] and [11], and validated in [12]. This model tries to develop two different behaviors in power grid system using the DC model:

1. **Slow dynamics**:A slow time scale, between days and years, is used in order to increase load and improve branch capacities.

2. **Fast dynamics**: In contrast, the blackout event unfolds using the result of the slow dynamics as a peak in load demand. The cascading events of a blackout take place in a faster time scale although the period of events is neglected.

The fast dynamics algorithm represents the blackout behavior therefore, there is no need to study slow dynamics. OPA fast dynamics explains in a very simple way how the control could interact in the blackout process. There are generation boundaries and using an optimization problem similar to the OPF model, the power flow problem and redispatch of power injection is calculated. Although, in this case Load Shedding is allowed. In this optimization the result is subject to the transmission line boundaries, and because Load Shedding is allowed there is always an optimal solution. However, in this model lines that are close to exceed their capacities are considered overloaded and could be cut.

The blackout is developed with this set of iterations below:

1. Line cut events are initiated according to a probability function as below:

$$\textbf{Probability line } j \textbf{ outaged} = h^0\left(\frac{f_j}{c_j}\right)$$

   Here h^0 is a positive and non-decreasing function. Then, if no lines are cut the iteration is finished.

2. The power injection is redispatched according to an optimization to minimize the change in generation and load shedding subject to DC model limits:

$$\begin{array}{rc} \textbf{minimize} & \sum_{i\in G}|p_i - p_{i0}| + \omega\sum_{i\in L}(p_i - p_{i0}) \\ \textbf{flow limits} & c_j = f_j^{max} \geq \left|f_j\right| \quad \forall i \in \mathscr{E} \\ & Mf = p \\ & Xf = M'\theta \\ \textbf{Bus i load limit} & 0 \geq p_i \geq p_{i0} \quad \forall i \in L \\ \textbf{Bus i gen limit} & p_i^{max} \geq p_i \geq 0 \quad \forall i \in G \\ \textbf{Reference bus} & \theta(\text{refbus}) = 0 \end{array}$$

   Here p_i^{max} is the maximum power injection of i generator bus. While ω is a high value in order to penalize load shedding from injection changes in generation buses. In all this report we will use $\omega = 100$, consistently with [8], [9], [10], [11], [12] and [13].

3. A line is considered overloaded when $f_j \geq 0.99c_j$ and will be cut with some probability:

$$\textbf{Probability overloaded line } j \textbf{ outaged} = h^1\left(\frac{f_j}{c_j}\right)$$

   Here h^1 is a positive and non-decreasing function.

4. If some line is cut in step 3 then step 4 is repeated. Therefore, if any line is not cut the fast dynamics breaking process is finished.

Improved OPA model

This model is developed as an improvement of the OPA model in [13]. The principal differences for this report are those developed in the fast dynamics. In this model, firstly the power flow solution is calculated as in the static model but is paid to attention to the maximum power injected in generators in the power injection redistribution. If any line is overloaded at this step there is a probability of using the OPA optimization. Therefore, this model tries to mix both models studied above. In addition the probabilities used in the OPA model in order to cut a line are changed in this model.

The blackout sequence is as below:

1. Initialization: Every transmission line has probability τ of being cut.

2. The DC power flow is calculated, and similar to the static model we do not take flow limits into consideration. Before this calculation, it is essential to redistribute power injection because the grid may be separated into several islands. If the total generation is greater than the total load, the power injection in generators is decreased in proportion to their initial condition. If the total generation is less than the total load, the active power generated is increased according to the reserve capacities. If the total generation capacity is less than the total demand, load shedding will be implemented in every load node proportional to its load amount. Therefore, in this case limits in power generation could cause load shedding.

3. If no line is overloaded the fast dynamics iteration is finished. However, if some line is overloaded the iteration continues.

4. With a probability ρ, the power injection is redispatched according to an optimization that minimizes the change in generation and load shedding subject to DC model constraints and flow limits. If $\rho = 1$ the optimization will be always done, if $\rho = 0$ it will be never done:

$$
\begin{array}{rc}
\textbf{minimize} & \sum_{i\in G}|p_i - p_{i0}| + \omega \sum_{i\in L}(p_i - p_{i0}) \\
\textbf{flow limits} & c_j = f_j^{max} \geq \left|f_j\right| \quad \forall i \in \mathscr{E} \\
 & Mf = p \\
 & Xf = M'\theta \\
\textbf{Bus i load limit} & 0 \geq p_i \geq p_i^{initial} \quad \forall i \in L \\
\textbf{Bus i gen limit} & p_i^{max} \geq p_i \geq 0 \quad \forall i \in G \\
\textbf{Reference bus} & \theta(\text{refbus}) = 0
\end{array}
$$

5. After the optimization in step 4 every transmission line has the $\delta\left|f_j/cj\right|^u$ probability formula in order to be tripped. u is considered with a value of 10.

If the optimization is not applied, then with the result of the second step any overloaded line is cut with a γ probability. The rest of the lines will also be tripped with a $\delta \left| f_j / cj \right|^u$ probability.

6. If some lines are cut in the last step then step 2 is repeated. If no line is cut the fast dynamics is finished.

Simplified improved OPA model

Given the models described above, we will decide upon one them in order to achieve our goals and use it in our simulations. The most complete model is the improved OPA model that tries to complement both the OPA and the Static model behaviors at the same time. Therefore, the iteration used in the simulations is the fast dynamics of the improved OPA model with some simplifications. This algorithm will be termed as the simplified improved OPA model. The full algorithm is described below:

1. Initialization: One line is selected to be cut.

2. At this point the power injection and withdrawal is redistributed. In point 3.1 this redistribution is explained. From this step a new p_{DC} array is developed for the next step.

3. The DC power flow is calculated:

$$\begin{gathered} Mf = p_{DC} \\ Xf = M'\theta \\ \theta(\text{refbus}) = 0 \end{gathered}$$

4. If no lines are overloaded $\forall j \in \mathscr{E} \quad c_j \geq f_j$ the blackout iteration is finished. In the other case continue.

5. The power injection is redispatched with a ρ probability according to an optimization to minimize the change in generation and load shedding subject to DC model constraints and flow limits:

$$\begin{array}{rc} \textbf{minimize} & \sum_{i \in G} |p_i - p_{i0}| + \omega \sum_{i \in L} (p_i - p_{i0}) \\ \textbf{flow limits} & c_j = f_j^{max} \geq \left| f_j \right| \quad \forall i \in \mathscr{E} \\ & Mf = p \\ & Xf = M'\theta \\ \textbf{Bus i load limit} & 0 \geq p_i \geq p_{i0} \quad \forall i \in L \\ \textbf{Bus i gen limit} & p_i^{max} \geq p_i \geq 0 \quad \forall i \in G \\ \textbf{Reference bus} & \theta(\text{refbus}) = 0 \end{array}$$

6. If the redispatch described in step 5 is done, an overloaded line will be considered when $0.99c_j \leq f_j$. But when the optimization is not done a line will be overloaded when $c_j \leq f_j$. All overloaded lines are cut depending on the next algorithm:

$$\forall(\text{overloaded line } j) \in \mathscr{E}$$

if $0.99c_j \leq f_j < c_j$ then

line j is cut with a probability of β

else if $f_j \geq c_j$ then

line j is cut with a probability of ξ

end

7. If some lines are disconnected in step 6 then, step 2 is repeated. Therefore, if any line is not cut the blackout iteration is concluded.

As is shown we have simplified the probabilities of cutting a transmission line. It is possible to select one line as the start of the branch breaking process. In addition, only the overloaded branches and the transmission lines that are close to their capacity could be cut in the development of the blackout.

3

Simulations

In this chapter some simulations are developed for two different bus systems using the simplified improved OPA model. The metrics explained above and two simple attacks described in this chapter are used in order to prevent blackouts. Firstly, we will describe how we use the bus system data and how the injection/withdrawal redistribution necessary in the simplified improve OPA model, works. After the simulations of each bus systems a discussion will describe the blackout and metrics results.

At this point we will simulate blackout activity on IEEE-14 and IEEE-96 RTS bus systems that can be found in [19]. In order to know if metrics are able to give us relevant information we will compare blackout results and metrics suggestions. In all the following simulations the probabilities used in order to cut overloaded transmission lines, β and ξ (step 6 of simplified improve OPA model), are 1, therefore, we will obtain the worst possible blackout results. Thereby, if any line is overloaded, it will be cut. In those systems, generators can have power injection and demand information. The power injected, considered for generator bus, is the difference between its injection and its demand, thereby if the power injected is less than the demand in a generator bus, this will be considered a load. In these bus systems the maximum power injected by generators is unknown, therefore, this value must be calculated using injection and demand in each generator as below:

$$\begin{aligned} p_{i0} &= -l_i & \forall i \in L \\ p_{i0} &= p_i - l_i & \forall i \in G \\ p_i^{max} &= \varpi\,(p_i - l_i) & \forall i \in G \end{aligned}$$

Here l_i and p_i are the demand and injection data from bus i respectively obtained from the bus system. While p_{i0} is the injection/withdrawal of the bus i and p_i^{max} is maximum possible power injected from the generator i respectively. ϖ is the constant value that represents the maximum injection a generator could inject using

the normal power injected by this bus. In both studied bus systems we do not have the maximum power injection, thus, we will always use $\varpi = 1.2$ assuming that all generators are able to support 20% more active power than in the normal state.

3.1 Redistribution of power injection and withdrawal

It is necessary to have a proper redistribution law when loads and generators are disconnected of the initial grid. This developed redistribution will be used in the second step of the simplified improved OPA algorithm shown in section 2.5.

When the blackout unfolds some loads, generators or both could be disconnected from the network. In other words, if some loads are not connected with any generator and/or some generators are not linked with any load bus then these nodes are disconnected from the entire network. It is understood that if a set of linked loads and generators is disconnected from the initial network, the grid evolves into two sets of networks with generators and loads. Let $\mathscr{I}$ be an island of graph $\mathscr{G}$. Hence, in each island the power generation and load demand is computed with this simple algorithm:

$$\forall \mathscr{I} \in \mathscr{G}$$

$$\text{if} \quad \left(-\sum_{i \in L \cap \mathscr{I}} p_{i0} > \sum_{i \in G \cap \mathscr{I}} p_i^{max}\right) \quad \text{then}$$

$$p_{iDC} = p_{i0} - p_{i0} \frac{-\sum_{j \in L \cap \mathscr{I}} p_{j0} - \sum_{j \in G \cap \mathscr{I}} p_j^{max}}{-\sum_{j \in L \cap \mathscr{I}} p_{j0}} \qquad \forall i \in L \cap \mathscr{I}$$

$$p_{iDC} = p_i^{max} \qquad \forall i \in G \cap \mathscr{I}$$

$$\text{else if} \quad \left(-\sum_{i \in L \cap \mathscr{I}} p_{i0} \leq \sum_{i \in G \cap \mathscr{I}} p_i^{max}\right) \quad \text{then}$$

$$p_{iDC} = p_{i0} \qquad \forall i \in L \cap \mathscr{I}$$

$$p_{iDC} = p_{i0} + p_i \frac{-\sum_{j \in L \cap \mathscr{I}} p_{j0} - \sum_{j \in G \cap \mathscr{I}} p_{j0}}{\sum_{j \in G \cap \mathscr{I}} p_j} \qquad \forall i \in G \cap \mathscr{I}$$

$$\text{end}$$

3.2 IEEE-14 bus system

IEEE-14 bus system is a 14 bus power grid with 5 generators, 9 load buses and 20 transmission lines. Branch impedances and bus nominal demands and injections are known. Maximum power injection in generator buses and transmission line capacities are not given. Zero nominal power is injected in generator buses 3, 6 and 8, therefore, they will be considered as loads. Generator 1 and 2 inject all the demand.

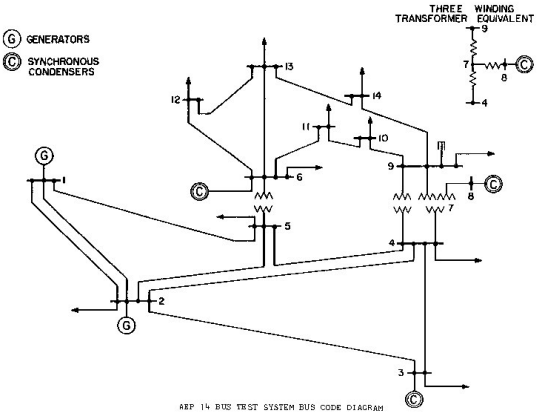

Figure 3.1 IEEE-14 bus system used in order to simulate blackouts [24]

In this system, transmission lines are unknown. In other assessments as [15] they obtain the capacities using a constant value called tolerance value. Firstly, the nominal power flow for each line is calculated using the DC power flow problem as follows:

$$\begin{gathered} Mf_0 = p_0 \\ Xf = M'\theta \\ \theta(\text{refbus}) = 0 \end{gathered}$$

Furthermore, the tolerance value υ is used to calculate the transmission line capacities as below:

$$c_j = \upsilon \left| f_{j0} \right| \quad \forall j \in \mathscr{E}$$

Capacities in power grids do not depend only on the nominal power flow of their branches and cut securities are normalized. Therefore, it is common to see a lot of transmission lines with the same capacities and different nominal power flows. Obviously those capacities are always higher than the nominal power flow in each branch. Hence, another possibility in order to apply capacities could be to decide 4 capacity values and apply them depending on the power flow of each branch. In this case we decided as in Table 3.1. In the following simulations we will use both concepts in order to obtain the appropriate capacities, therefore, we could get more information.

Number line	From bus- To bus	Nominal flow	Capacity
1	1-2	149.53	250
2	1-5	71.44	100
3	2-3	69.99	100
4	2-4	55.11	100
5	2-5	40.75	100
6	3-4	-24.20	50
7	4-5	-62.50	100
8	4-7	28.98	50
9	4-9	16.62	50
10	5-6	42.09	100
11	6-11	6.31	20
12	6-12	7.54	20
13	6-13	17.04	50
14	7-8	0.0	20
15	7-9	28.98	50
16	9-10	6.19	20
17	9-14	9.92	20
18	10-11	-2.81	20
19	12-13	1.44	20
20	13-14	4.98	20

Table 3.1 IEEE-14 bus system capacities used in the simulations. The nominal power flow is calculated using the DC power flow model. We decided to use this 4 capacity values depending on the nominal power flow.

IEEE-14 bus system simulations

Firstly, we are going to use different tolerance values υ and show which metric could find the worst possible blackout. Therefore, below in Figure 3.2 we can show the worst blackout result (orange and blue) and the average of all possible blackouts cutting an individual line (red) for each tolerance value using $\rho = 0$ and $\rho = 1$. The load shedding LS can have values from 0 to 1 as shown in the normalize Equation (2.5). A bigger load shedding will present a more critical blackout.

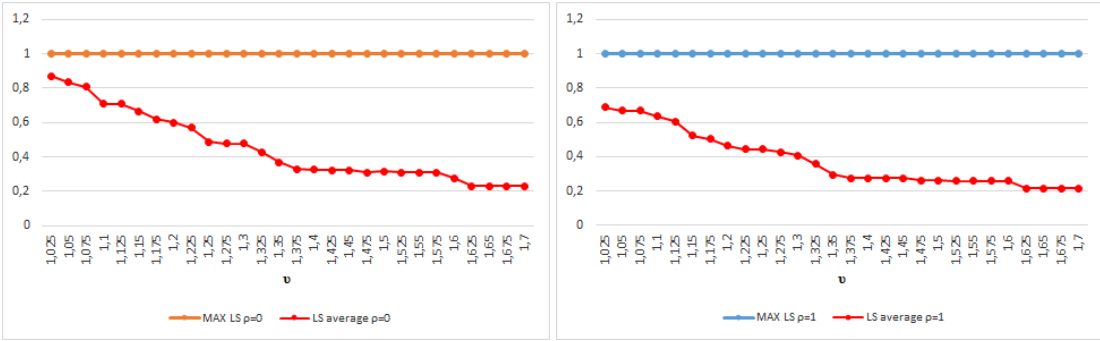

Figure 3.2 "MAX LS" is the maximum LS obtained cutting one line and "LS average" is the LS average obtained cutting all the transmission lines. The y-axis represent the load shedding resulted from a blackout and the x-axis represent the tolerance value υ. The left figure represents the case when $\rho = 0$ and the right one represents the case when $\rho = 1$. The load shedding average decrease with the increase of tolerance value and the results using $\rho = 1$ are less critical.

The capacities increase uniformly with the tolerance value, therefore, the metrics result will always be the same. The next table shows which line is the most critical for each metric:

Metric	Elec. Bet.	Eff. Res.	Net-ability
Line cut	8	10	7

Table 3.2 IEEE-14 bus system critical lines suggestion for each metric

We can also apply other kind of attacks in order to obtain the worst blackout:

Node significance: Cut the most important branch of the most significant node. Thus, cut the line connected to the bus with highest injection/withdrawal (in absolute value), where nominal power flow is higher than the rest of the edges connected to this bus.

Highest power flow: Cut the line with the largest nominal power flow level.

Attack	Node sign.	Highest pow.
Line cut	1	1

Table 3.3 IEEE-14 bus system critical lines suggestion for each attack

The following figures show the LS result for υ values between 1.025 and 1.7, for $\rho = 0$ and $\rho = 1$, and for the different cut lines depending on the metric used in each case. This figures show the individual branch cut that each metric suggested in Table 3.2, where in Figure 3.2 is presented the average of all branch cuts, for every tolerance value.

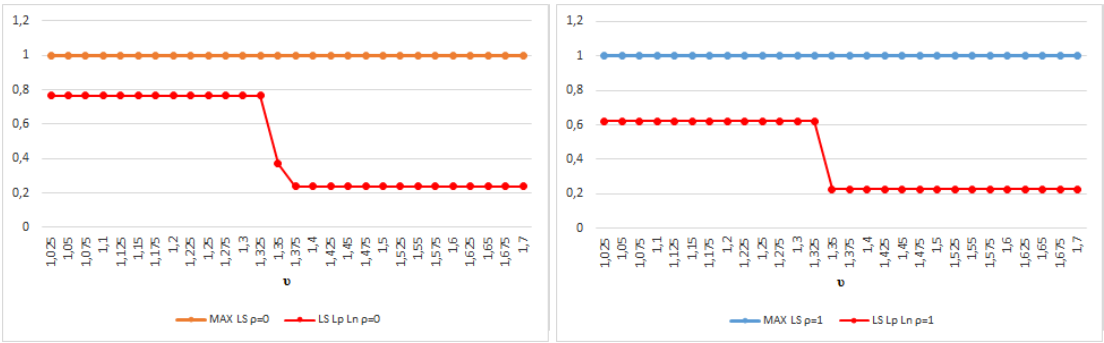

Figure 3.3 "MAX LS" is the maximum LS obtained cutting one line and "LS Lp Ln" is the LS obtained cutting the transmission line pointed by the electrical betweenness metric. The y-axis represent the load shedding resulted from a blackout and the x-axis represent the tolerance value υ. The left figure represents the case when $\rho = 0$ and the right one represents the case when $\rho = 1$. There is a tolerance value where the cut on this particular branch get less critical.

Figure 3.3 shows less critical load shedding using $\rho = 1$ in coherence with Figure 3.2. In addition, in coherence Figure 3.2, there is a tolerance value where a cut on this particular branch get less critical.

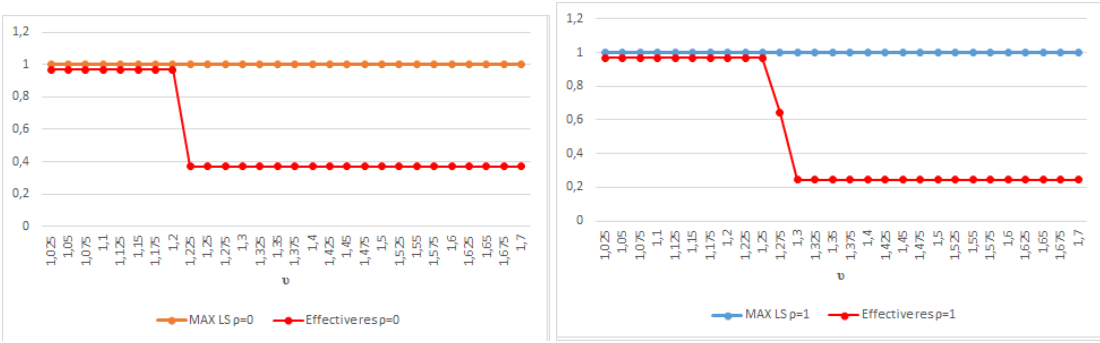

Figure 3.4 "MAX LS" is the maximum LS obtained cutting one line and "Effective res" is the LS obtained cutting the transmission line pointed by the effective resistance metric. The y-axis represent the load shedding resulted from a blackout and the x-axis represent the tolerance value υ. The left figure represents the case when $\rho = 0$ and the right one represents the case when $\rho = 1$. In this case with $\upsilon = 1.225$ and $\upsilon = 1.25$ we get less critical load shedding using $\rho = 0$.

In Figure 3.4 we see that for $\upsilon = 1.225$ and $\upsilon = 1.25$ we get less critical load shedding using $\rho = 0$. These are some of the exceptions where $\rho = 1$ obtain worst blackout results. In general with $\rho = 0$ blackouts results are worst as shown in Figure 3.2. For the rest of the tolerance values we obtain equal or worst results using $\rho = 0$.

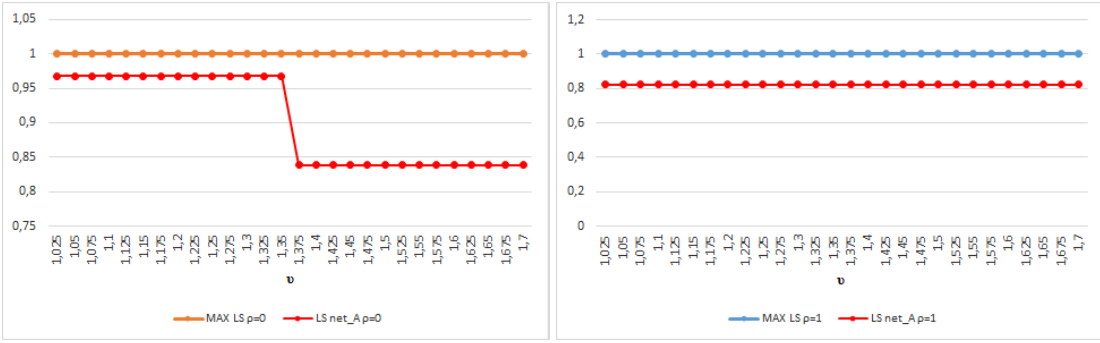

Figure 3.5 "MAX LS" is the maximum LS obtained cutting one line and "LS net_A" is the LS obtained cutting the transmission line pointed by the net-ability metric. The y-axis represent the load shedding resulted from a blackout and the x-axis represent the tolerance value υ. The left figure represents the case when $\rho = 0$ and the right one represents the case when $\rho = 1$. With $\rho = 1$ the same load shedding is obtained. In addition for $\rho = 0$ the *LS* is always worst and with a little descend at $\upsilon = 1.375$ similar to the figures above.

Figure 3.5 unfolds that with $\rho = 1$ the same load shedding is obtained. In addition for $\rho = 0$ the LS is always worst and with a little descend at $\upsilon = 1.375$ similar to the figures above. This is the metric with worst blackouts for all tolerance values.

The same transmission line is selected in Table 3.3 using the above explained attacks. For every tolerance value and ρ value (0 and 1) the load shedding resulting from cutting branch 1 is $LS = 0.899$. Therefore, the worst blackouts are unfold by these attacks and the net-ability metric. However, any of them obtain the worst possible blackout.

As is shown in Figure 3.2 the LS average results using $\rho = 1$ are better than using $\rho = 0$, therefore, we will use $\rho = 0$ in the following simulations in order to obtain the worst scenario. In the last simulation of the IEEE 14 bus system we will use the capacities listed in Table 3.1 and increase the demand and injection until one line is close to exceeding its capacity. Therefore, we increase demand and injection 35% and we simulate for each branch cut a blackout. Table 3.4 shows the transmission lines ordered by its blackout LS results and by the different metrics and attacks compared in this report. In red are colored those transmission lines that have unfold the worst blackouts.

Nº line	LS	Elec. Bet.	Eff. Res.	Net-ability	Node sign.	Highest pow.
2	1	1	10	1	1	1
3	1	4	16	7	2	2
4	1	2	15	4	3	3
5	1	5	17	5	6	7
7	1	10	8	2	7	4
10	0.9679	8	11	3	4	10
1	0.8991	3	18	6	8	5
6	0.3969	7	20	10	9	8
9	0.3696	6	13	8	15	15
8	0.2397	15	1	15	17	6
15	0.2397	9	6	16	16	13
13	0.1454	13	19	11	5	9
17	0.0628	16	12	18	20	17
20	0.0628	11	7	17	13	12
11	0	17	9	20	19	11
12	0	18	3	13	10	16
14	0	20	2	9	12	20
16	0	12	4	12	11	18
18	0	19	5	19	18	19
19	0	14	14	14	14	14

Table 3.4 IEEE-14 bus system ordered transmission lines depending on the LS blackout results and, metrics and attacks suggestions. The most critical lines are colored red. Therefore, the electrical betweenness metric, the net-ability metric and the highest power flow attack are the best capturing the most critical lines in the upper part of the table. The effective resistance metric has the worst results predicting the critical branches with five of these lines in the bottom.

IEEE-14 bus system discussion

In the first simulations, we can see that, with higher tolerance values υ, blackout results are better. In average we obtain better *LS* results using $\rho = 1$. No attack or metric has obtained the worst result. However, the node significance and highest power flow attacks have the worst results for all the tolerance values. Net-ability has also high *LS* results. Furthermore, between effective resistance and electrical betweenness it seems that we obtain worse blackouts using the effective resistance.

With the data obtained from the first simulation, we can only obtain which attack unfolds the worst blackout. However, in the second simulation Table 3.4 shows which attack or metric has the worst possible blackouts as first options. Therefore, it is shown that the electrical betweenness, the net-ability and the highest power flow attack have seven of the worst blackouts as first options. Node significance attack

has good results, however branch 5 and 10 are far from the rest of the critical attacks. Finally, the effective resistance does not obtain the critical transmission lines in the correct order.

3.3 IEEE-96 RTS bus system

IEEE-RTS-96 bus system is a 72 buses power grid that can be divided into 3 identical power grids with 24 buses as below:

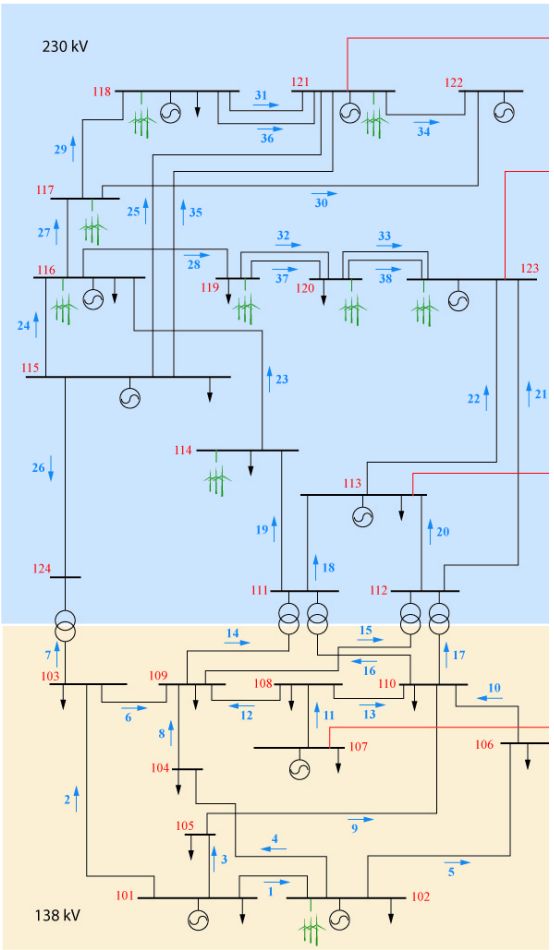

Figure 3.6 IEEE-RTS-96 24 buses used in order to simulate blackouts system [25]

This is a 24 bus system with 10 generators, 14 load buses and 39 transmission lines. Branch impedances and capacities as well as bus nominal demands and injections are known. Maximum power injection in generator buses is unknown. In this case we have lines capacities data, although these branch limits are measured in MVA. Generators 13 and 15 have less power injection than withdrawal , therefore,

they will be considered as loads. In this grid the most important generators are in the upper part. Buses 15 and 13 are considered loads, therefore, the inferior part of the grid is full of loads. The power flow will go from the upper part to the inferior part in order to fill the demand.

We do not have the maximum power injection, therefore, it will be calculated using $\varpi = 1.2$ as written above . It will be considered the worst blackout case using $\rho = 0$ in our simulations. The capacities are in MVA and not in MW and the peak of demand is represented by a 10% increase, hence, in order to do the simulations the demand will also be increased by 20%. A 10% increase would represent the reactive power in transmission lines, thereby, we could use the capacities as MW values. In addition, as written above, the other 10% increase will represent a more stressed grid.

Another simulation case will be represented with an increase until one transmission line is close to exceeding its own capacity. This case is produced with a 50% increase, therefore we will have 2 simulations using the IEEE-96 RTS bus system: one with 20% and the other with 50% demand/injection increase.

From this bus system we also have the number of times a transmission line is cut per year. This value can be useful in order to calculate which could be the most critical, not only using the damage a transmission line can cause, but its probability of being cut.

IEEE-96 RTS bus system simulation

In the case with a 20% increase the power grid has an N-1 security, thus, if we only cut one transmission line a blackout will never occur. Therefore, we will cut one line and recalculate another one using the metrics and attacks described until we obtain a blackout. As written above, from the IEEE-96 RTS bus system we obtain the probability for each line to be cut in a year. Although we do not have the probability of having a combination of several cut lines, we approximate that the sum of these probabilities could reflect this possibility. Furthermore, the product of this value and the LS blackout result could be used as an efficiency number. This will be called "attack efficiency". When this number is higher the more efficient the attack is:

$$\text{attack efficiency} = \begin{pmatrix} \text{sum of the probabilities} \\ \text{for each line to be cut} \end{pmatrix} * \begin{pmatrix} \text{The } LS \text{ resulted from the blackout} \\ \text{unfolded by these branch cuts} \end{pmatrix}$$

Attacks	Electrical Betweenness	Net-ability	Effective Resistance
Attacked lines	30-24-31	30-24-31	27-6
Load Shedding	0.3093	0.3093	0.6352
Attack efficiency	0.3217	0.3217	0.5017

Attacks	Node significance	Highest power flow
Attacked lines	21-22	23-22
Load Shedding	0.6352	0.6352
Attack efficiency	0.6415	0.6097

Table 3.5 IEEE-RTS-96 24 buses power grid attack and metrics results. The electrical betweenness and net-ability metrics did not obtain as critical combinations as the remaining attacks and metric.

Table 3.5 shows different cuts developed by the metrics and attacks studied, and their results. Attack efficiency values from combination of 2 cuts cannot be compared with the 3 cuts combinations. Moreover, it is important to compare these values with the best possible attacks for each combination. In order to do that we have simulated all the 2 and 3 transmission line cut combinations that generate a blackout. In the following histograms we can see the number of attacks that cause blackouts with similar results of LS and attack efficiency:

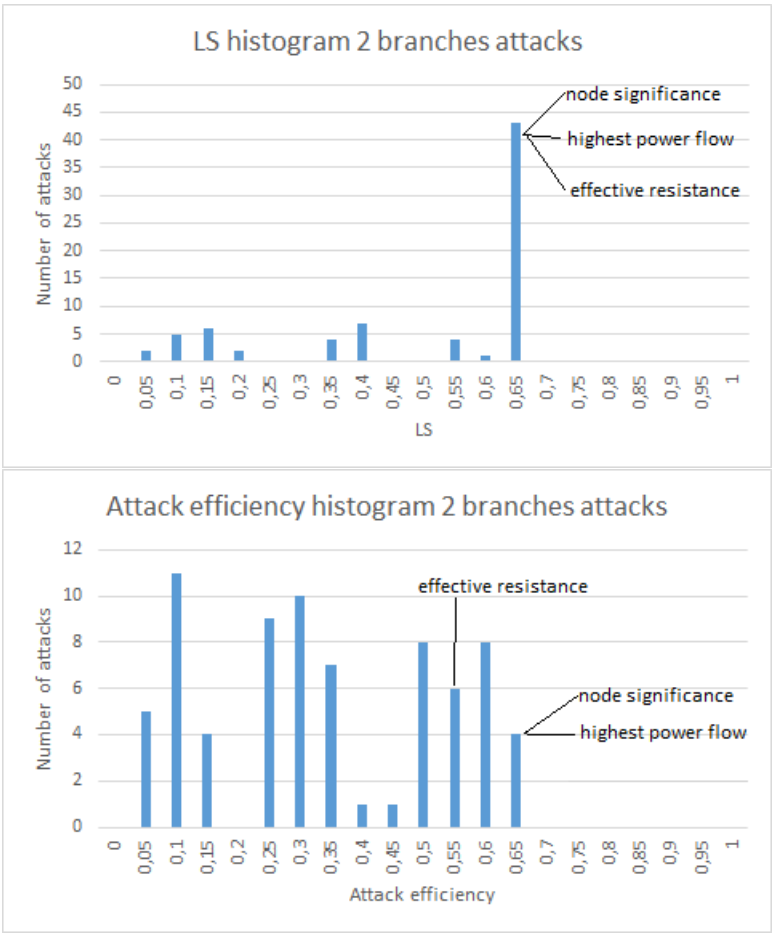

Figure 3.7 Histogram that clusters the 2 branch combination attacks where their LS and attack efficiency results are similar. These attacks and metric get some of the most critical 2 branch combinations.

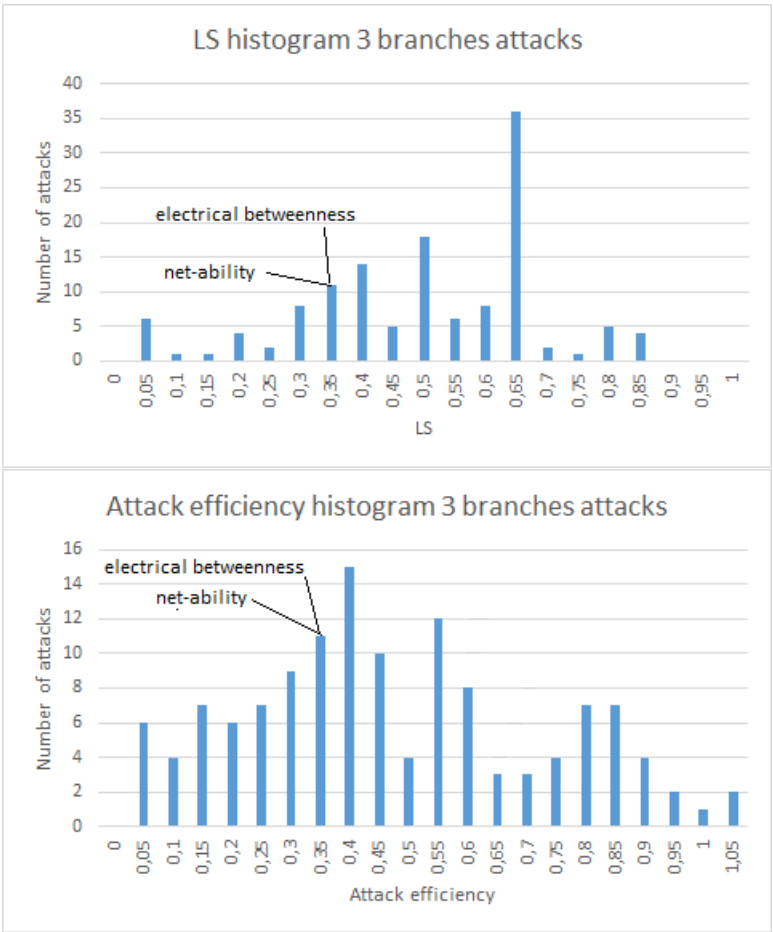

Figure 3.8 Histogram that clusters the 3 branch combination attacks where their LS and attack efficiency results are similar. These metrics did not get some of the most critical 3 branch combinations.

In both cases, two and three branch cuts, we can find the worst blackout results, depending on the attack efficiency. These attacks can be used to compare with the metric results:

Attacks	Attack(2) 1	Attack(2) 2	Attack(2) 3	Attack(2) 4
Attacked lines	2-27	21-23	21-27	27-32
Load Shedding	0.6352	0.6352	0.6352	0.6352
Attack efficiency	0.5843	0.6288	0.591	0.6034

Table 3.6 IEEE-RTS 96 24 bus system worst attack results for 2 branch combination cuts

Attacks	Attack(3) 1	Attack(3) 2	Attack(3) 3	Attack(3) 4
Attacked lines	3-5-22	21-36-37	22-36-37	26-36-37
Load Shedding	0.7535	0.8329	0.8329	0.8329
Attack efficiency	0.9795	1.0328	1.0078	0.9412

Table 3.7 IEEE-96 RTS 24 bus system worst attack results for 3 branch combination cuts

As written above, we will simulate the IEEE-96 RTS bus system with a 50% demand/injection increase. In this scenario the grid loses its N-1 security. Therefore, we will order transmission lines by its blackout LS and attack efficiency results. Branches will also be ordered by the different metrics and attacks compared in this report. The following tables compare the critical lines by *LS* and efficiency attack with the critical lines by using the metrics and attacks described. In red are colored the most critical branches depending on the *LS* or the attack efficiency respectively:

Nº line	LS	Elec. Bet.	Eff. Res.	Net-ability	Node sign.	Highest pow.
25	0.8329	30	27	30	21	23
26	0.8329	23	10	29	22	28
22	0.6910	29	12	24	36	21
7	0.6351	19	13	23	37	22
11	0.6351	28	8	19	39	7
17	0.6351	27	7	39	25	27
21	0.6351	22	19	27	26	25
23	0.6351	21	1	28	38	26
27	0.6351	39	23	7	33	30
29	0.6351	25	9	22	32	17
18	0.5914	26	29	21	31	38
5	0.0807	7	4	36	17	31
10	0.0807	24	3	37	16	16
1	0.0	38	2	25	10	15
2	0.0	31	24	26	13	19

Table 3.8 IEEE-96 RTS bus system ordered transmission lines depending on the LS blackout results and, metrics and attacks conclusions. The complete tables can be found in Appendix A Table A.1 and Table A.2 as the first and the second part of this table respectively. Colored in red the most critical branches. The highest power flow attack and the electrical betweenness metric obtain most of the critical branches in the upper part, followed by the net-ability metric. The worst result is obtained with the effective resistance suggestion.

Nº line	Attack eff.	Elec. Bet.	Eff. Res.	Net-ability	Node sign.	Highest pow.
26	0.3415	30	27	30	21	23
22	0.3386	23	10	29	22	28
21	0.3303	29	12	24	36	21
23	0.2985	19	13	23	37	22
11	0.2748	28	8	19	39	7
27	0.2604	27	7	39	25	27
18	0.2366	22	19	27	26	25
29	0.2223	21	1	28	38	26
17	0.1905	39	23	7	33	30
5	0.0387	25	9	22	32	17
10	0.0266	26	29	21	31	38
7	0.0127	7	4	36	17	31
17	0.0127	24	7	37	16	16

Table 3.9 IEEE-96 RTS bus system ordered transmission lines depending on the attack efficiency blackout results and, metrics and attacks conclusions.The complete table can be found in Appendix A Table A.3. Colored in red the most critical branches. The highest power flow attack and the electrical betweenness metric obtain most of the critical branches in the upper part, followed by the net-ability metric. The worst result is obtained with the effective resistance suggestion.

IEEE-96 RTS bus system discussion

In the first simulations, where a combination of branch cuts is necessary in order to unfold blackouts, node significant attack, highest power flow attack, and effective resistance metric obtain some of the more *LS* than the remaining metrics. However, this is not enough to consider this 3 attacks as the most critical. These three methods have also high attack efficiency compared with the remaining two branch cut combinations. Furthermore, we compare these results with other four severe attacks in Table 3.6. As written above, the power flow must go from the upper part to the inferior part in order to fill the demand. Therefore, the worst results could happen when lines in the superior and the middle part are cut.

Furthermore, we compare line cuts in Table 3.6 and two branch cuts in Table 3.5. Lines 2 and 6 are in the inferior part, lines 27 and 32 are in the superior part, and lines 21, 22 and 23 connect the inferior and superior part. Therefore, there are two of these attacks that combine the attack through the transmission line 27 with branch 2 or 6. Hence, this precise attack in the left-inferior side could redirect the power flow to the right-inferior side and generate a big blackout. Node significance metric and highest flow attack seem to disconnect middle lines that are crucial to redistribute the active power through the inferior part.

The net-ability and the electrical betweenness metrics represent the same line cuts and must be compared with the three branch cut combinations that develop a blackout. In this case, three of the worst attacks are based on cutting branches 36 and 37. Furthermore, a big blackout unfolds cutting intermediate lines 26, 22 or 21. In Attack(3) 1, two branches in the inferior part and one line in the middle part are cut. Disconnecting lines 3 and 5 could make it more easier for other lines in the inferior part to overload, here the capacities are lower than in the upper part of the grid. Moreover, cutting the middle transmission line 22 a blackout is developed. Net-ability and electrical betweenness did not suggest some of the worst 3 branch cut combinations. However, the attacks are based on the same tactic as written above: two attacks in the superior part and one in the intermediate part.

In Table A.1 highest power flow attack and electrical betweenness metric have branches better ordered. Followed by net-ability metric. Effective resistance metric seems to have less similitudes with the worst results. Finally, node significance attack only obtains transmission lines 21, 22, 25 and 26 in the superior part of its list. In Table A.3 the electrical betweenness metric, the net-ability metric and the highest power flow attack maintain in the upper part the most of the critical branches. In addition the effective resistance metric and the node significance attack does not obtain the critical branches correctly ordered.

4

Conclusion

The studied metrics can not always obtain as the first option the most critical branch that can unfold a blackout. However, electrical betweenness and net-ability metrics obtain the critical branches within the first options. The highest power flow attack also obtains similar results. Therefore, they capture the critical transmission lines in order to unfold blackouts. Then, it might be possible in future assessments to combine net-ability and electrical betweenness metrics with the nominal power flow in each line. Hence, those lines that carry high levels of power flow could have higher weighed metric results not only depending on these metrics, but on its power flow levels.

However, lines that carry a high amount of power flow are usually more protected than others, thereby, those branch cuts are improbable. It could be necessary to study those lines that carry less power flow and are less protected but are more probable to unfold a critical blackout. Thereby, the probability of having a single line cut or a combination of line cuts will be useful in future assessments. Introduce these values in metrics might help them to be more precise in their results. A transmission line will be more critical not only when it can generate huge damage, but it has higher probabilities to being cut.

The effective resistance metric did not obtain all the critical branches within its first suggestions. Therefore, the effective resistance is not capable of capturing the critical branches of the power grid. In summary, electrical betweenness and net-ability metrics have good results looking for the weakness of a power grid, however, these metrics need to be improved in order to use them in blackout prevention systems. As written above the real probability of being cut is another important parameter in transmission lines criticality.

A

Complete tables

Table A.1 and Table A.2 are the first and the second part of the complete Table 3.8 respectively. Where Table A.3 is the complete Table 3.9.

Nº line	LS	Elec. Bet.	Eff. Res.	Net-ability	Node sign.	Highest pow.
25	0.8329	30	27	30	21	23
26	0.8329	23	10	29	22	28
22	0.6910	29	12	24	36	21
7	0.6351	19	13	23	37	22
11	0.6351	28	8	19	39	7
17	0.6351	27	7	39	25	27
21	0.6351	22	19	27	26	25
23	0.6351	21	1	28	38	26
27	0.6351	39	23	7	33	30
29	0.6351	25	9	22	32	17
18	0.5914	26	29	21	31	38
5	0.0807	7	4	36	17	31
10	0.0807	24	3	37	16	16
1	0.0	38	2	25	10	15
2	0.0	31	24	26	13	19
3	0.0	3	16	38	9	18
4	0.0	18	30	18	23	36
6	0.0	17	6	31	19	37
8	0.0	16	17	34	29	11

Table A.1 IEEE-96 RTS bus system ordered transmission lines depending on the LS blackout results and, metrics and attacks conclusions. First part of the complete table of Table 3.8.

Nº line	LS	Elec. Bet.	Eff. Res.	Net-ability	Node sign.	Highest pow.
9	0.0	36	38	35	34	14
12	0.0	37	21	1	35	10
13	0.0	34	39	20	7	29
14	0.0	35	5	2	6	24
15	0.0	6	28	17	2	32
16	0.0	20	22	16	15	33
19	0.0	9	14	6	14	39
20	0.0	1	15	15	12	3
24	0.0	4	18	8	8	20
28	0.0	32	31	4	11	5
30	0.0	33	20	14	5	34
31	0.0	15	25	32	27	35
32	0.0	14	26	33	24	12
33	0.0	2	32	3	4	8
34	0.0	5	33	9	18	4
35	0.0	8	34	10	20	6
36	0.0	11	35	5	1	13
37	0.0	10	36	12	3	2
38	0.0	13	37	13	30	1
39	0.0	12	11	11	28	9

Table A.2 IEEE-96 RTS bus system ordered transmission lines depending on the LS blackout results and, metrics and attacks conclusions. Second part of the complete table of Table 3.8.

Nº line	Attack eff.	Elec. Bet.	Eff. Res.	Net-ability	Node sign.	Highest pow.
26	0.3415	30	27	30	21	23
22	0.3386	23	10	29	22	28
21	0.3303	29	12	24	36	21
23	0.2985	19	13	23	37	22
11	0.2748	28	8	19	39	7
27	0.2604	27	7	39	25	27
18	0.2366	22	19	27	26	25
29	0.2223	21	1	28	38	26
17	0.1905	39	23	7	33	30
5	0.0387	25	9	22	32	17
10	0.0266	26	29	21	31	38
7	0.0127	7	4	36	17	31
17	0.0127	24	7	37	16	16
1	0.0	38	2	25	10	15
2	0.0	31	24	26	13	19
3	0.0	3	16	38	9	18
4	0.0	18	30	18	23	36
6	0.0	17	6	31	19	37
8	0.0	16	17	34	29	11
9	0.0	36	38	35	34	14
12	0.0	37	21	1	35	10
13	0.0	34	39	20	7	29
14	0.0	35	5	2	6	24
15	0.0	6	28	17	2	32
16	0.0	20	22	16	15	33
19	0.0	9	14	6	14	39
20	0.0	1	15	15	12	3
24	0.0	4	18	8	8	20
28	0.0	32	31	4	11	5
30	0.0	33	20	14	5	34
31	0.0	15	25	32	27	35
32	0.0	14	26	33	24	12
33	0.0	2	32	3	4	8
34	0.0	5	33	9	18	4
35	0.0	8	34	10	20	6
36	0.0	11	35	5	1	13
37	0.0	10	36	12	3	2
38	0.0	13	37	13	30	1
39	0.0	12	11	11	28	9

Table A.3 IEEE-96 RTS bus system ordered transmission lines depending on the attack efficiency blackout results and, metrics and attacks conclusions. Complete table of Table 3.9.

Bibliography

[1] J.J.Grainger , W.D.Stevenson Jr., “Power system analysis”,McGraw-Hill Series in Electrical and Computer Engineering, Editions 1994, Chapter-9, 329-376.

[2] R.D.Zimmerman, C.E.Murillo-Sánchez, “MATPOWER 5.1 User’s Manual”, Power Systems Engineering Research Center, December 20, 2015, Chapter-4, 28-32.

[3] E.Bompard, E.Pons, D.Wu, “Extended Topological Metrics for the Analysis of Power Grid Vulnerability”, IEEE SYSTEMS JOURNAL, VOL-6, NO- 3, September 2012, 481-487.

[4] S.Arianos, E.Bompard, A.Carbone, F.Xue, “Power grid vulnerability: A complex network approach”, CHAOS, 19, 013119, 20 February 2009, 1-6.

[5] L.Cuadra, S.Salcedo-Sanz, J.Del Ser, S.Jiménez-Fernández, Z.Woo Geem, “A Critical Review of Robustness in Power Grids Using Complex Networks Concepts”, Energies, 2015, 8, 9211-9265.

[6] Y.Koç, M.Warnier, R.E.Kooij, F.M.T.Brazier , “Structural Vulnerability Assessment of Electric Power Grids”, arXiv:1312.6606v1 [physics.soc-ph], 19 Dec 2013.

[7] Yakup Koç, Martin Warnier, Piet Van Mieghem, Robert E. Kooij, Frances M.T. Brazier , “The Impact of the Topology on Cascading Failure in a Power Grid Model”, Physica A: Statistical Mechanics and its Applications, Volume 402, 15 May 2014, 169–179.

[8] B.A.Carreras, V.E.Lynch, I.Dobson, D.E.Newman, “An Initial model for complex dynamics in electric power system blackouts”, in System Sciences, 2001. Proceedings of the 34th Annual Hawaii International Conference on System Sciences, pp.710-718, 6-6 Jan. 2001.

[9] B.A.Carreras, V.E.Lynch, I.Dobson, D.E.Newman, “Modeling Blackouts Dynamics in Power Transmission Networks with Simple Structure”, in System Sciences, 2001. Proceedings of the 34th Annual Hawaii International Conference on System Sciences, pp.719-727, 6-6 Jan. 2001.

[10] B.A.Carreras, V.E.Lynch, I.Dobson, D.E.Newman, "Dynamics, Criticality and Self-organization in a Model for Blackouts in Power Transmission Systems", in System Sciences, 2002, HICSS, Proceedings of the 35th Annual Hawaii International Conference on System Sciences, pp.9 pp.-, 7-10 Jan. 2002.

[11] B.A.Carreras, V.E.Lynch, I.Dobson, D.E.Newman, "Critical points and transitions in an electric power transmission model for cascading failure blackouts",CHAOS, VOLUME 12, NUMBER 4, December 2002, 985-994.

[12] B.A.Carreras, N.S.Degala, I.Dobson, D.E.Newman "Validating OPA with WECC data",in System Sciences (HICSS), 2013 46th Hawaii International Conference on System Sciences, pp.2197-2204, 7-10 Jan. 2013.

[13] S.Mei, F.He, X.Zhang, S.Wu, G.Wang "An Improved OPA Model and Blackout Risk Assessment", IEEE TRANSACTIONS IN POWER SYSTEMS, VOL.24, NO.2 , May 2009, 814-823.

[14] D.Kirschen, G.Strbac "Why investments do not prevent blackouts", The Electricity Journal, Volume 17, Issue 2, March 2004, Pages 29–36.

[15] Y.Koç, T.Verma, N.A.M.Araujo, M.Warnier "MATCASC:A tool to analyse cascading line outages in power grids", arXiv:1308.0174v1 [physics.soc-ph] 1 Aug 2013.

[16] S.Pahwa, C.Scoglio, A.Scala "Abruptness of Cascade Failures in Power Grids", Scientific Reports 4, Article number: 3694 (2014).

[17] P.Hines, K.Balasubramaniam, E.Cotilla Sanchez "Cascading Failures in power grids", in Potentials, IEEE , vol.28, no.5, pp.24-30, September-October 2009.

[18] "Learning from the blackouts", IEA PUBLICATIONS December, 2005, Chapter 2, Case Study 3: Sweden and Denmark, 90-99.

[19] University of Washington Electrical Engineering Power Systems Test Case Archive "http://www.ee.washington.edu/research/pstca/" 10-01-2016.

[20] C.Lai, S.H.Low, "The Redistribution of Power Flow in Cascading Failures", in Communication, Control, and Computing (Allerton), 2013 51st Annual Allerton Conference, pp.1037-1044, 2-4 Oct, 2013.

[21] S.H.Low, "Convex Relaxation of Optimal Power Flow—Part I: Formulations and Equivalence", IEEE Transactions on Control of Networks Systems, vol. 1 issue 1, pages 15-27, 2014.

[22] K. Savla, G. Como, and M.A.Dahleh, "Robust Network Routing under Cascading Failures", IEEE Transactions on Network Science and Engineering, vol. 1, issue 1, pages 53-66, 2014.

[23] J.A. Taylor, "Convex Optimization of Power Systems", Cambridge University Press, 2015.

[24] IEEE-14 bus system picture, "*http://www.ee.washington.edu/research/pstca/pf14/pg_tca14fig.htm*", 10 Dec, 2016.

[25] IEEE-RTS-96 bus system picture, "*http://www.ee.washington.edu/research/real/Library/Data/IEEE-RTS_3.jpg*", 10 Dec, 2016.

Lund University
Department of Automatic Control
Box 118
SE-221 00 Lund Sweden

Document name
MASTER´S THESIS

Date of issue
January 2016

Document Number
ISRN LUTFD2/TFRT--5997--SE

Author(s)
Nicolás Bordonaba Mateos

Supervisor
Carolina Lidström, Dept. of Automatic Control, Lund University, Sweden
Giacomo Como, Dept. of Automatic Control, Lund University, Sweden
Bo Bernhardsson, Dept. of Automatic Control, Lund University, Sweden (examiner)

Sponsoring organization

Title and subtitle

On cascading failure models and robustness metrics in power networks

Abstract

Network research tries to give solutions within several areas, beginning from social interconnections, logistic problems, virus spreading, supply networks...etc. Some metrics have been developed in order to predict blackouts and improve power grid robustness. Metrics use part of the grid information seeking weakness without simulating the blackout process. On the other hand, simulation models unfold blackouts.

In this report, we study such metrics and models, seeking that model that could give us the most relevant information. The models studied in this report represent blackout as a branch breaking process, a singular line cut or a combination of line cuts might cause subsequent disconnections and unfold a blackout. The IEEE-14 and IEEE-96 RTS bus systems are used in order to simulate blackouts. Metrics suggestions are compared with the simulations in these grids in order to know which metric better captures the critical branches.

None of the studied metrics turns out to indicate always the worst blackout result as the first option. In addition, the results suggest that the effective resistance metric did not predict the critical transmission lines of the grid. Electrical betweenness and net-ability metrics obtain the critical transmission lines within their first suggestions. However, the results might be better if we also use other relevant information on the grid as the nominal power flow in each branch or the probability of having a line cut. Nevertheless, lines that carry a high amount of power flow are usually more protected and more difficult to being cut and develop a blackout. The probability of having a single line cut or a combination of line cuts will be useful in future assessments in order to seek not only the most critical branch cuts, but the most probable ones.

Keywords

Classification system and/or index terms (if any)

Supplementary bibliographical information

ISSN and key title
0280-5316

ISBN

Language
English

Number of pages
1-61

Recipient's notes

Security classification